Journal of Anatomy

J. Anat. (2016) doi: 10.1111/joa.12525

Anatomical study of the auditory region of *Arctotherium tarijense* (Ursidae, Tremarctinae), an extinct short-faced bear from the Pleistocene of South America

Maria Eugenia Arnaudo,[1] Paula Bona,[1] Leopoldo Hector Soibelzon[1] and Blaine W. Schubert[2]

[1]*División Paleontología de Vertebrados-CONICET, Museo de La Plata, La Plata, Argentina*
[2]*Center of Excellence in Paleontology and Department of Geosciences, East Tennessee State University, Johnson City, TN, USA*

Abstract

Here we present the most detailed morphological study of the auditory region of a tremarctinae bear, *Arctotherium tarijense* Ameghino. In addition, we provide new anatomical information of the Tremarctinae inner ear, such as coplanarity and deviation from orthogonality of the semicircular canals, as an approach to infer the head movements which encountered the extinct forms in locomotion. Based on morphological comparisons, *A. tarijense* exhibits the following particular features: the cavum tympani presents the highest relative volume compared with other ursids; the processus paraoccipitalis has a foramen that is absent in other tremarctines; there is only one (ventral) recess in the anterior region of the cavum tympani; and the recessus epytimpanicus is the smallest for all ursids studied. In relation to the inner ear, *A. tarijense* shows the lowest values of orthogonality deviation and highest scores of locomotor agility. Based on this, is possible to make a preliminary proposal that this species had a relative high vestibular sensibility and therefore a better ability to explore different kind of habitats. However, this hypothesis might be contrasted among bears taking into account the orientation of each semicircular canal in a phylogenetic framework.

Key words: *Arctotherium*; auditory region; locomotor agility; morphology; Ursidae.

Introduction

Traditionally, the auditory region in mammals has provided important information about three principal aspects: phylogeny (based on middle and inner ear features; e.g. Turner, 1848; Flower, 1869; Van Kampen, 1905; Pocock, 1921, 1922, 1929; Van Der Klaauw, 1931; Thenius, 1949; Hough, 1952; Ginsburg, 1966; de Beaumont, 1968; Hunt, 1974; Eisenberg, 1989; Wozencraft, 1989, 2005; Wyss & Flynn, 1993; see Arnaudo et al. 2014), hearing capacity, and locomotor behavior (Spoor & Zonneveld, 1998; Spoor, 2003; Schmelzle et al. 2007; Spoor et al. 2007; Silcox et al. 2009; Macrini et al. 2010; Malinzak et al., 2012; Billet et al. 2013).

Although soft tissues in general, and those related to the ear, are not preserved in fossil specimens, it is possible to study those structures by reconstructing them from the bony recesses and cavities that they filled. Inner ear elements are contained in the petrosal bone. The petrosal includes soft organs, such as the petrosal lobule of the cerebella paraflocculus (contained by the subarcuate fossa), the cochlea, the saccule, the utricle, and the semicircular ducts (contained by the bony labyrinth). The cochlea is the principal organ of hearing, whereas the other structures are associated with spatial orientation and balance (Macrini et al. 2010). Studies on the cochlea configuration require a detailed observation of anatomical structures [mostly based on micro-computed tomography (CT) scans] to infer hearing capacity (Macrini et al. 2010; Orliac et al. 2012; Billet et al. 2013; Ekdale, 2013; Rodrigues et al. 2013). On the other hand, the best understood function of the semicircular canal system is its contribution to the stabilization of gaze during locomotion (Spoor & Zonneveld, 1998; Spoor, 2003; Spoor et al. 2007). The system works to integrate optic flow, i.e. the changes in the retinal images that occur when moving and that are important clues in sensing distance as well as body position. Stabilization is accomplished via the vestibuloocular and vestibulocollic reflexes that involve,

Correspondence
Leopoldo Hector Soibelzon, División Paleontología de Vertebrados-CONICET, Museo de La Plata, Paseo del Bosque s/n, 1900, La Plata, Argentina. E: lsoibelzon@fcnym.unlp.edu.ar

Accepted for publication *23 June 2016*

when moving, the extraocular and neck muscles, respectively. The 'canonical model' of semicircular canal orientation in mammals assumes that corresponding left and right canal pairs present angle symmetry, the three ipsilateral canals are disposed in orthogonal planes (i.e. orthogonality), left and right canals pairs have equivalent angles (i.e. angle symmetry), and contralateral synergistic canals occupy parallel planes (i.e. coplanarity). However, species often diverge substantially from this model and those with more orthogonal semicircular canals tend to have higher mean vestibular sensitivity than those with less orthogonal semicircular canals (Berlin et al. 2013).

The petrosal lobule of the cerebella paraflocculus cross-references information regarding head and eye position during voluntary and reflex eye movements. Together with other factors, such as endolymph viscosity and the duct lumen size, the arc size of the enclosed duct influences the mechanical response behavior of the semicircular canal system (Spoor & Zonneveld, 1998). Several authors have proposed a strong link between locomotor patterns and semicircular canal size in extant species, giving an interesting tool for assessing locomotor behavior in related extinct taxa, independent of that inferred from their postcranial skeleton (e.g. Spoor & Zonneveld, 1998; Spoor et al. 2007; Walker et al. 2008; Silcox et al. 2009; Ryan et al. 2012).

In Ursinae (Carnivora, Ursidae) the auditory region has been studied in different extant and fossil species (e.g. Segall, 1943; Hough, 1948; Davis, 1964; Torres, 1984, 1987, 1988), but in Tremarctinae it is practically unknown, with the exception of the description of *Arctotherium angustidens* provided by Arnaudo et al. (2014). Tremarctinae bears are distributed exclusively in the Americas (Soibelzon et al. 2005) with four genera: *Plionarctos* and *Arctodus* (distributed in North America), *Arctotherium* (distributed in South America) and *Tremarctos* (distributed in both North and South America); represented by small (e.g. *Arctotherium wingei*, *Tremarctos ornatus*) and gigantic species (e.g. *Arctodus simus, Arctotherium angustidens*) recorded from the late Miocene (*Plionarctos*) to recent times (Kurtén, 1966, 1967; Tedford & Martin, 2001; Soibelzon, 2004; Soibelzon et al. 2005; Schubert, 2010; Soibelzon & Schubert, 2011).

Within *Arctotherium*, *A. tarijense* is a medium- to small-sized species (Soibelzon & Tartarini, 2009; Soibelzon & Schubert, 2011; Table 1) known from the Bonaerian and Lujanian Ages (middle Pleistocene to early Holocene). *Arctotherium angustidens* (Early to Middle Pleistocene) and *Arctotherium bonariense* (Middle Pleistocene) are the largest species of the genus, and *A. wingei* (Late Pleistocene) (Soibelzon et al. 2005; Soibelzon & Tartarini, 2009) the smallest. Here we focus on the auditory region (external, middle, and inner ear) of *A. tarijense* Ameghino, 1902, describing the morphological variation and exploring paleobiological implications.

Institutional abbreviations

CIMED: Centro de Imágenes Médicas. GP: Museu Paulista, Universidad de San Pablo, Brazil. H: Illinois State Museum, USA. MACN: Museo Argentino de Ciencias Naturales, Buenos Aires, Argentina. MHJ: Museo Histórico de Junín, Argentina. MLP: Museo de La Plata, División Paleontología Vertebrados, La Plata, Argentina. MLP DZV: Museo de La Plata, Departamento de Zoología, La Plata, Argentina. MMP: Museo Municipal de Mar del Plata 'Lorenzo Scaglia', Mar del Plata, Argentina. MMPH: Museo Municipal 'Punta Hermengo', Miramar, Argentina. TMM: Texas Memorial Museum, USA. UF: University of Florida, Gainesville, USA. USNM: United States National Museum, USA.

Table 1 Body mass, range of locomotor agility scores (mean value in bold), measurements of the canalis semicircularis, middle ear volume of Arctotherium tarijense and the other Ursidae used for comparisons. There were estimated for those taxa from which CT scans were obtained. Body mass is given as an average of CR4, CR5 and CR6 (Van Valkenburgh, 1990).

Species	Collection number	BM (kg)	Agility	CSAR (mm)	CSPR (mm)	CSLR (mm)	CSR (mm)	Middle ear vol. (mm^3)
Arctotherium tarijense	MACN 971	231.0984	2.72–2.88 **(2.82)**	3.75	3.57	2.87	3.396	11902.47
Arctotherium angustidens	MLP 82-X-22-1	743.5703	2.10–2.80 **(2.26)**	3.54	3.07	3.55	3.386	11380.72
Tremarctos ornatus	MLP 1-I-03-62	85.13114	2.16–2.81 **(2.61)**	2.19	2.26	2.326	2.258	1366.4
Tremarctos ornatus	MLP 2329	85.763	2.34–2.85 **(2.42)**	2.45	2.75	2.37	2.523	1523.3
Ursus spelaeus	MLP 10-69	546.122	2.30–2.81 **(2.55)**	3.37	3.495	3.18	3.4325	8342.3
Ursus maritimus	H 001-05	637.1702	2.19–2.35 **(2.21)**	3.439	3.368	2.802	3.203	3592.79
Ursus maritimus	USNM 275072	307.0434	2.4–2.75 **(2.58)**	3.808	3.123	2.920	3.284	4366.51
Ursus americanus	USNM 227070	123.7801	2.13–2.5 **(2.29)**	2.91	2.53	1.84	2.426	2289.195
Ursus arctos	TMM M-2749	139.3864	2.35–2.78 **(2.56)**	2.743	2.74	2.531	2.671	4090.83
Ursus arctos	USNM 98062	145.0101	2.63–2.66 **(2.63)**	3.262	3.008	2.399	2.890	2620.875

Materials and methods

Specimens

All known specimens of *A. tarijense* with a preserved auditory region were studied. This includes MACN 971 (holotype of *Pararctotherium pamparum* Ameghino, synonymized to *A. tarijense* by Soibelzon, 2004), MHJ 544, and MLP 10-5. MACN 971 (Fig. 1A–C) is a complete and well-preserved cranium. The specimen MHJ 544 (Fig. 1D–F) is also a complete skull but has a lot of carbonate deposition outside and even inside the skull, with several foramina and the inner ear observed on CT scans; specimen MLP 10-5 (Fig. 1G–I) is represented by a large cranial fragment that comprises the basicranium and occipital bones. Micro CT scans could not be obtained, so it was not possible to make any hearing capacity inferences based on the cochlear configuration.

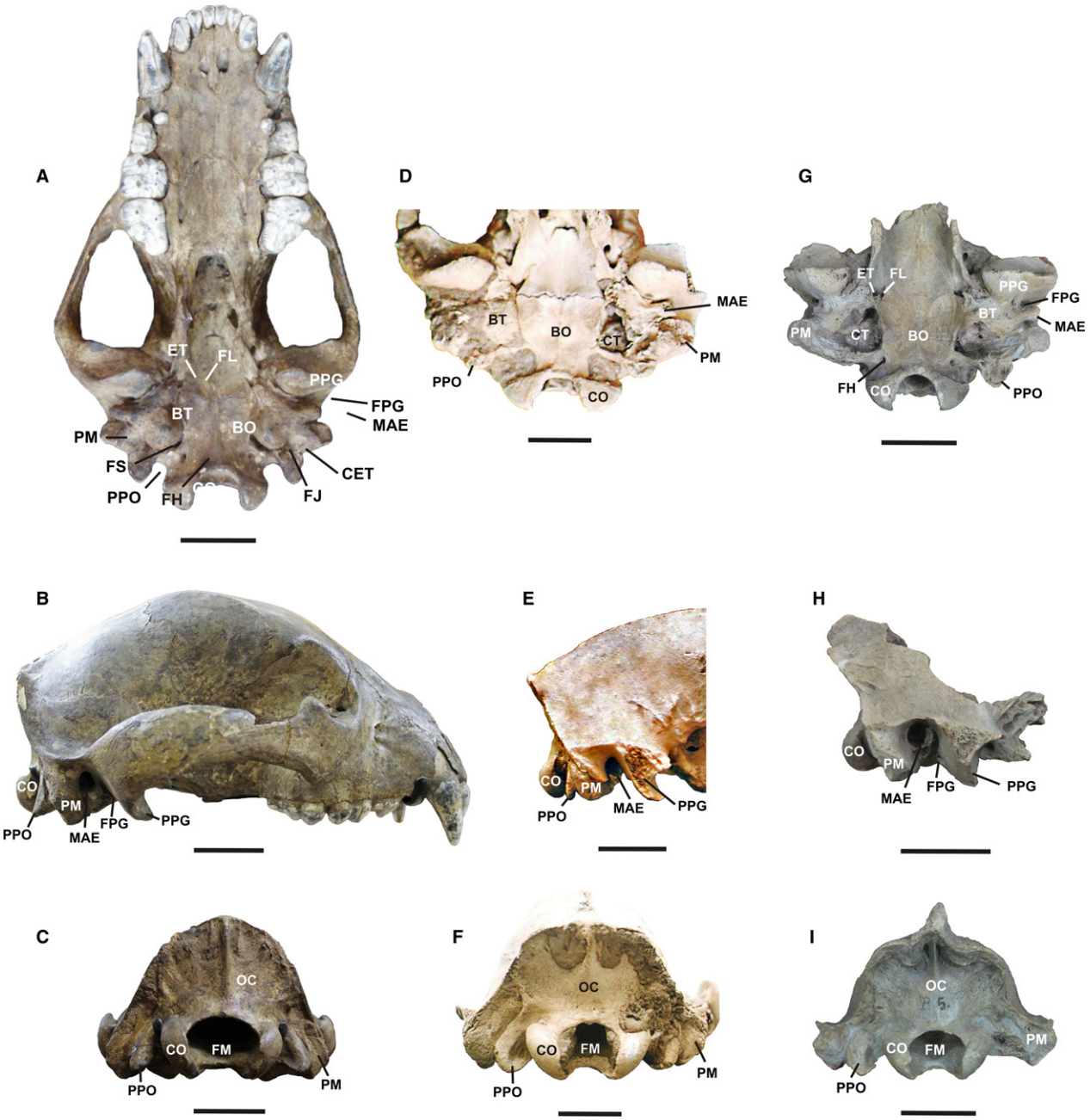

Fig. 1 *Arctotherium tarijense*. (A–C) MACN 971. A, Ventral; B, lateral; C, occipital views of the skull; (D–F) MHJ 544. D, Ventral; E, lateral; F, occipital views of the braincase; (G–I) MLP 10-5. G, Ventral; H, lateral; I, occipital views of the braincase. BO, pars basilaris os occipitale; BT, bulla tympanica; CET, contact exoccipital-bulla tympanica; CO, condylus occipitalis; ET, Eustachian tube; FH, foramen n. hypoglossis; FJ, foramen jugulare; FL, foramen lacerum; FM, foramen magnum; FPG, foramen postglenoideum; FS, foramen stylomastoideum; MAE, meatus acusticus externus; PM, processus mastoideus; PPG, processus postglenoideus; PPO, processus paraoccipitalis; OC, os occipitale. Scale bar: 5 cm.

Material used for comparisons were examined by M.E.A. and L.H.S. and include: *A. angustidens* (MACN 43, MACN 5132, MACN 974, MLP 82-X-22-1, MACN 12529, MMP 1491M, MMP 1232, MLP 10-4, MLP 00-VII-10-1, MLP 00-VII-15-1, MMP 3981, MMP 3982, MMMP 26S, MMP 162S, MMPH 018); *A. bonariense* (MLP 00-VII-1-1) and *Tremarctos ornatus* (MLP DZV 1-I-03-62 and MLP DZV 2329). *Arctotherium wingei* (GP/2E 04) was studied from pictures. For comparisons of the internal cavities of *A. tarijense*, we used CT scans of *Ursus arctos* (TMM M-2749, USNM 98062), *Ursus americanus* (USNM 227070), and *Ursus maritimus* (H 001-05, USNM 275072) provided by the Digital Morphology library at The University of Texas at Austin (www.digimorph.org). In addition, the CT scans of *A. angustidens* (MLP 82-X-22-1), *A. bonariense* (MLP 00-VII-1-1) and *T. ornatus* (MLP DZV 1-I-03-62 and MLP DZV 2329) were generated in a private institution (CIMED, La Plata, Buenos Aires) with a Philips/Brilliance 64 Scanner, at 120 kV, with a slice thickness of 0.670 mm. The CT scans of *T. floridanus* (UF 7454) and *A. pristinus* (UF 154288) were provided by Franklin Woods Community Hospital in Johnson City, Tennessee. These last CT scans were made with a Siemens/Somatom Definition AS Scanner, with a slice thickness of 0.6 mm.

Morphological analysis

For anatomical descriptions, we follow the Nomina Anatomica Veterinarium (2012) and specific terminology used for bears by Davis (1964) and Torres (1987). Comparisons of the external morphology of the auditory region were carried out through direct observation. The analysis of the internal morphology of the middle and inner ear were made by 3D reconstructions made with the free version of the 3D Slicer Software 4.3.1; this software was also used to estimate the skull and the bulla tympanica volumes. This is a non-invasive method to study internal anatomical structures. *Arctotherium tarijense* was studied by means of CT scans and 3D reconstructions of specimen MACN 971. The middle ear volume was reconstructed considering the recessus epytimpanicus, the recessus where the canalis facialis opens and the fosae for the muscles tensor tympani and stapedialis. In this species these are small cavities in relation to the total volume of the bulla.

Linear measurements of the inner ear were obtained using MeshLab 1.3.4 (http://meshlab.sourceforge.net) directly from the 3D model following Schmelzle et al. (2007). The inner ear model was oriented with the canalis semicircularis lateral (CSL) in the horizontal plane when taking measurements of the canalis semicircularis anterior and posterior (CSA and CSP, respectively); the CSA was oriented horizontally when measuring the CSL (Schmelzle et al. 2007; Spoor et al. 2007; Macrini et al. 2010; Billet et al. 2013). The height of the canalis semicircularis is always defined as the largest distance of the arc from the vestibule; the width is perpendicular to the height, irrespective of the orientation of the canal in the skull (Spoor & Zonneveld, 1998). For this, we measured the length of the arch (described by each canalis semicircularis) from the inner border of the canals (Schmelzle et al. 2007) farthest away from the vestibule and the width of the arch (of each semicircular canal) was measured perpendicular to its length (Schmelzle et al. 2007). Measurements were taken three times and the mean value calculated. The radius of curvature (R) of each canal was calculated using the following equation: $[0.5(l + w)/2]$ where l = is the length of the canal and w = the width of the canal (Spoor & Zonneveld, 1998).

Predicting head movements and locomotion

To make the angle comparisons, stable head-centered reference planes are required, especially for angle comparisons of contralateral canals. To orientate the head, we used bilateral measurements of Reid's line [extending from the lower edge of the orbit to the center of the aperture of the external auditory canal to define the horizontal/frontal plane (XY)]. The axial (YZ) plane contained the line connecting the two external auditory meatuses (interaural line) perpendicular to the frontal and sagittal reference planes (Berlin et al. 2013). To calculate deviations from orthogonality, deviation from side-to-side semicircular canal angle symmetry and to quantify deviation from coplanarity, we followed Berlin et al. (2013).

To infer aspects related to locomotion in extinct tremarctines, the results of the head movement analysis were compared with the locomotor agility estimated for fossil and recent tremarctines, *Ursus spelaeus* and extant ursines, using the equation proposed by Silcox et al. (2009), based on the measurements of the semicircular canals.

$$\text{CSAR: } \log_{10}\text{AGIL} = 0.850 - 0.153\,(\log_{10}\text{BM}) + 0.706\,(\log_{10}\text{CSAR})$$
$$\text{CSPR: } \log_{10}\text{AGIL} = 0.881 - 0.151\,(\log_{10}\text{BM}) + 0.677\,(\log_{10}\text{CSPR})$$
$$\text{CSLR: } \log_{10}\text{AGIL} = 0.959 - 0.1670\,(\log_{10}\text{BM}) + 0.854\,(\log_{10}\text{CLSR})$$
$$\text{CSR: } \log_{10}\text{AGIL} = 0.948 - 0.188\,(\log_{10}\text{BM}) + 0.962\,(\log_{10}\text{CSR})$$

where AGIL = agility; CSAR = canalis semicircularis anterior radius; BM = body mass in grams; CSLR = canalis semicircularis lateral radius; CSPR = canalis semicircularis radius; CSR = average canalis semicircularis radius.This equation was developed using a dataset obtained by Spoor et al. (2007) based on qualitative field information on extant mammals. Spoor et al. (2007) assigned locomotor agility scores for a sample of 210 mammal species on a scale of 1–6, with 1 being extremely slow and 6 fast. Recently, the use of locomotor agility scores has been under a high degree of scrutiny and there is controversy surrounding the use of locomotor agility scores to infer locomotor capabilities of extinct taxa (Malinzak et al. 2012; Berlin et al. 2013; Ekdale, 2016).

To orientate the 3D skull models, the CSL has been considered parallel to the horizontal plane (see Blanks et al. 1972; Spoor & Zonneveld, 1998; Witmer et al. 2003). But CSL is not considered a good indicator of the position of the head in life (as an indicator of the horizontal plane, e.g. Berlin et al. 2013). However, in *A. tarijense*, the CSL are likely coplanar (together, they form an angle of 8; Table 2). Also, we estimated the skull orientation for *A. angustidens*, *A. bonariense*, *T. ornatus, T. floridanus*, and *A. pristinus* to make comparisons.

The body mass of MACN 971 and of the other ursids used for comparisons (see Table 1) were estimated following three equations described by Van Valkenburgh (1990) that were used earlier by Soibelzon & Tartarini (2009). These equations are based on the occiput-to-orbit length:

$$\text{CR4: } \log y = 3.44 * \log x - 5.74$$
$$\text{CR5: } \log y = 1.98 * \log x - 2.38$$
$$\text{CR6: } \log y = 1.51 * \log x - 1.25$$

where CR4 is the equation for Carnivora, CR5 for Ursidae, and CR6 for species in size category above 100 kg (see Van Valkenburgh, 1990).

Each mass value was adjusted according to its respective standard error (SE) (*sensu* Smith, 1993) and the arithmetic mean then calculated.

Table 2 Orientation of each six semicircular canals: 90_{var} (average orthogonality deviation), coplanarity, angle symmetry, angles between ipsilateral canals (IPS) and synergic semicircular canals (SYN).

	Arctotherium tarijense	*Arctotherium angustidens*	*Arctotherium Bonariense*	*Tremarctos ornatus*	*Tremarctos floridanus*	*Arctodus pristinus*
90_{var}	4.90	9.22	6.90	4.71	7.12	4.73
Coplanarity	16.55	13.03	8.33	20.71	4.55	–
Angle symmetry	7.6	9.7	2.68	0.38	5.85	–
RCSA-RCSP IPS	75.71	103.97	87.72	91.54	84.61	93.65
RCSP-RCSL IPS	91.12	98.45	98.45	89.11	90.77	90.91
RCSA-RCSL IPS	87.79	77.76	81.77	78.57	78.17	80.36
LCSA-LCSP IPS	89.25	95.85	90.04	92.03	95.64	–
LCSP-LCSL IPS	89.1	85.35	102.96	88.74	91.50	–
LCSA- LCSL IPS	80.53	69.62	80.54	78.85	72.38	–
LASC-RPSCSYN	18.84	13.34	15.88	36.35	8.13	–
LPSC-RASC SYN	21.92	17.02	3.63	22.3	4.54	–
LLSC-RLSC SYN	8.9	8.74	2.49	3.19	1.09	–

RCSA, Right canalis semicircularis anterior; RCSP, right canalis semicircularis posterior; RCSL, right canalis semicircularis lateral; LCSA, left canalis semicircularis anterior; LCSP, left canalis semicircularis posterior; LCSL, left canalis semicircularis lateral; see Material and methods.

Description

External morphology of the auditory region

The ventral, lateral and posterior views of the braincase of *A. tarijense* are shown in Fig. 1. In occipital view the processus mastoideus (anterolaterally oriented in this species) is extended more ventrally than the processus paraoccipitalis (*sensu* Davis, 1964), which is posteriorly oriented, with a sharp apex (Fig. 1B). In two of the three speciemens, the processus mastoideus is wider than the condyles occipitalis, whereas the processus paraoocipitalis is relatively small. However, in MLP 10-5 the condyles occipitalis are wider than the other two structures (Fig. 1C,F,I).

The ectotympanic (tympanic) and entotympanic bones (*sensu* Hunt, 1974) are fused forming a single bone, as in *A. angustidens* and other mammals (Arnaudo et al. 2014). This bone forms the bulla tympanica and the meatus acusticus externus (Fig. 1A,D,G). In lateral view, in MLP 10-5 and MHJ 544, the bulla tympanica barely approaches the processus mastoideus, ventrally. This condition is present on the left side of the bulla of MACN 971, whereas on the right side the bulla tympanica exceeds the processus mastoideus ventrally. The meatus acusticus externus is elliptical in longitudinal section, anterolaterally oriented, and it dorsal wall is distally opened. It is separated from the processus postglenoideus anteriorly and the processus mastoideus posteriorly by deep sulci. In all known specimens of *A. tarijense* the foramen postglenoideus is also visible in the lateral view and it is located anterior to the meatus acusticus externus (Fig. 1, see A,D,G). In MACN 971 this foramen is partially covered by a small crest formed by the tympanic, whereas in MLP 10-5 this crest is absent (Fig. 1A–H).

In ventral view (Fig. 1A,D,G), the meatus acusticus externus does not laterally surpass the processus mastoideus. At the anteromedial edge of the bulla tympanica lies the foramen lacerum that joins together the openings of Eustachian tube (lateral) and canalis caroticus (medial). This foramen is partially covered by an anterior expansion of the auditory bulla. Posteromedial to the bulla tympanica are the foramen jugulare (for the passage of the nervi glossopharyngeus, nervi vagus, nervi accessorius and the venae jugularis) and the canalis caroticus (placed anterior to the former), for the passage of arteria carotis interna. Lateral to both foramina opens the foramen stylomastoideum (for the passage of the nervi facialis, the ramus auricularis of the nervi vagus and the arteria stylomastoidea) (Davis, 1964). The foramen jugulare and the canalis caroticus are separated from the foramen stylomastoideum by a conspicuous ridge that connects the processus paraoccipitalis with the bulla tympanica. In *A. tarijense* there is a small foramen at the medial base of the processus paraoccipitalis, probably for the passage of a cranial nerve branch. Medial to this foramen is the foramen n. hypoglossis, which connects with the canalis n. hypoglossi (XII) and it is placed in the fossa condylaris ventralis. The bulla tympanica contacts medially with the pars basilaris of the os occipitale, which in this species does not overlap the bulla.

Middle ear

The middle ear volume of MACN 971 is 11902.33 mm^3. The cavum tympani is narrower and taller than in *A. angustidens* (Fig. 2). Its medial, lateral and ventral walls are formed by the bulla tympanica. This cavity is delimited by the pars petrosa of the os temporale, dorsally. This pars conforms

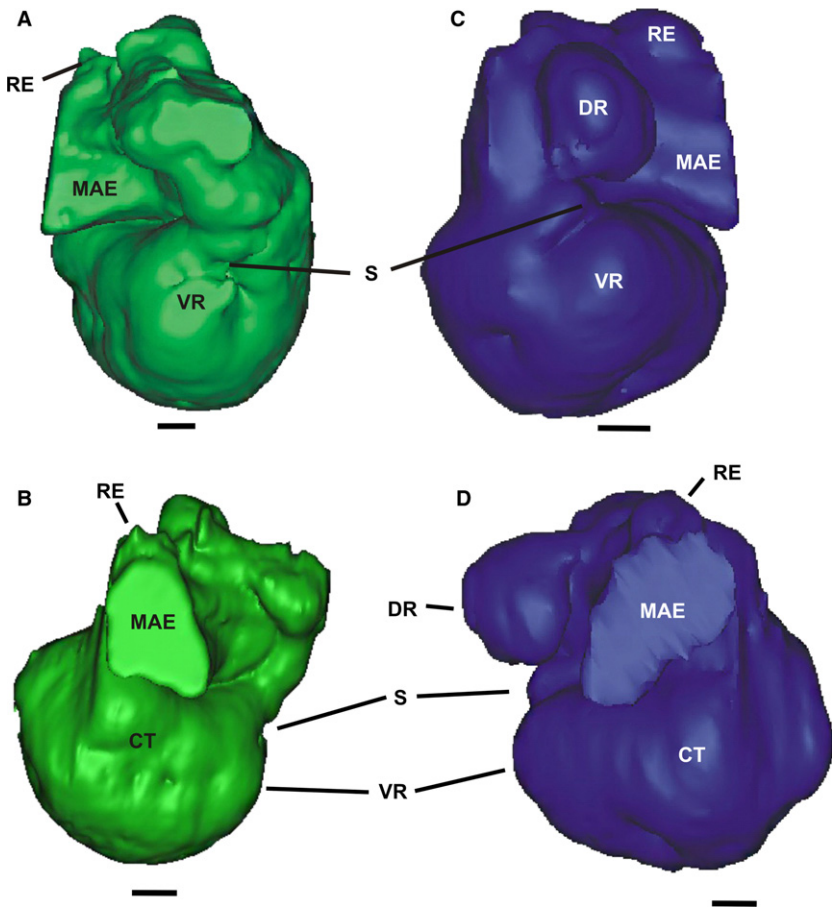

Fig. 2 Three-dimensional reconstruction of the middle ear. (A,B) *Arctotherium tarijense* (MACN 971). (C,D) *Arctotherium angustidens* (MLP 82-X-22-1). A, anterior and B, lateral views of the right cavum tympani; C, anterior and D lateral views of the left cavum tympani. CT, cavum tympani; DR, dorsal recess; MAE, meatus acusticus externus; RE, recessus epytimpanicus; S, septum; VR, ventral recess. Scale bar: 5 cm.

the processus mastoideus that is anteriorly oriented (see below). At the anterior wall of the cavum tympani there is a smooth horizontal septum that delimits an incipient ventral recess, whereas the dorsal recess, present in other species (i.e. *A. angustidens*), is absent (Fig. 2). As in other bears, in *A. tarijense* the curve ridges (transverse ridges *sensu* Torres, 1987) are hardly visible in the lateral and ventral walls of the cavum tympani (Arnaudo et al. 2014).

The canalis caroticus is placed on the medial wall of the cavum tympani, below the pars petrosa of the os temporale (Fig. 3B,C); given its location it is probably completely formed by the entotympanic (Arnaudo et al. 2014).

Dorsal to the meatus acusticus externus is the small chamber where the malleus and the incus articulate. This chamber corresponds to the recessus epitympanicus, which in MACN 971 is smaller than that of *A. angustidens* and other tremarctines (e.g. *A. bonariense* and *T. ornatus*) (Figs 2 and 3B).

The pars petrosa of the os temporale is placed medial to the meatus acusticus externus with the promontorium as the most prominent part. The fenestra cochleae (posteroventral to the promontorioum) and fenestra vestibuli (anterolateral to the promontorium) are preserved (Fig. 3C, D). The fenestra vestibuli contacts the footplate of the stapes in life.

Inner ear

The pars petrosa of the os temporale is shown in the Fig. 4. The three semicircular canals of MACN 971 were reconstructed (Fig. 5). The area of the arc comprising the canalis semicircularis posterior (CSP) and canalis semicircularis lateral (CSL) are oval, whereas the area of the arc enclosed by the canalis semicircularis anterior (CSA) is rounded (Fig. 5). Each canalis semicircularis joins the utriculus through its ampullae (Ladevèze et al. 2008), but in MACN 971 we were unable to reconstruct these structures. The CSP forms a crus commune with the CSA and, as in other bears, in MACN 971 an secondary crus commune is also observed (Arnaudo et al. 2014) (Fig. 5A,B). This secondary crus commune is composed by the posterior part of the CSL and the inferior part of the CSP; therefore, the canalis semicircularis reaches the utriculus by means of only four openings (Cox, 1962; Meng & Fox, 1995; Sánchez-Villagra & Schmelzle, 2007; Ladevèze et al. 2008, 2010; Ruf et al. 2009; Ekdale & Rowe, 2011; Luo et al. 2011, 2012). The CSP is posteroventral to the CSA, which is posterodorsally to anteroventrally oriented. The CSL is anterodorsally to posteroventrally oriented. The CSP and the CSA are the same height, as is typical for quadruped species (Schmelzle et al. 2007) (Fig. 5).

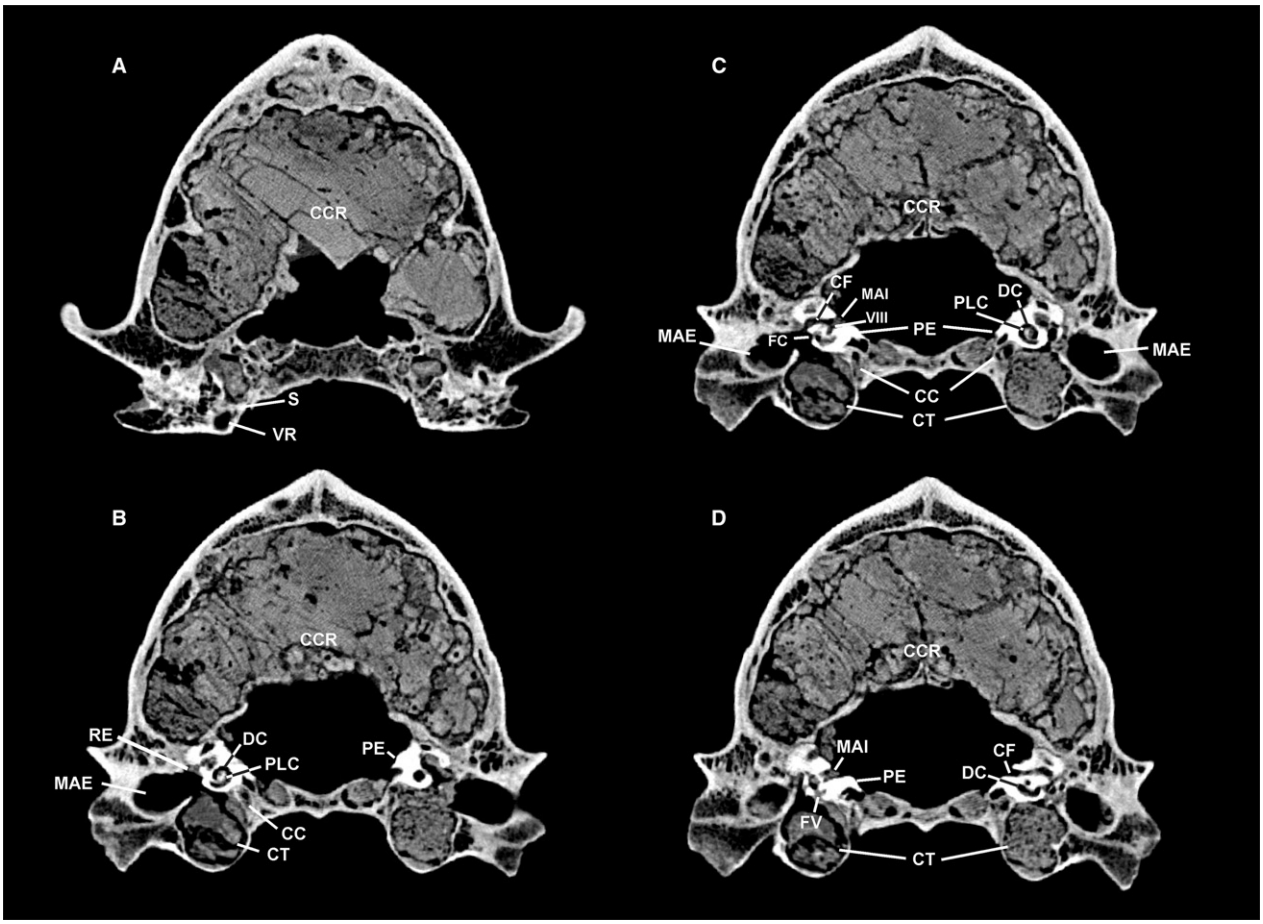

Fig. 3 CT coronal images of the skull of *A. tarijense* (MACN 971). (A–D) from anterior to posterior. CC, canalis caroticus; CCR, cavum cranii; CF, canalis facialis; CT, cavum tympani; DC, ductus cochlearis; FC fenestra cochleae; FV, fenestra vestibuli; MAE, meatus acusticus externus; MAI, meatus acusticus internus; PLC, primary lamina of the cochlea; RE, recessus epytimpanicus; PE, pars petrosa os temporale; VIII, opening for the nervi vestibulocochlearis; VR, ventral recess; S, septum.

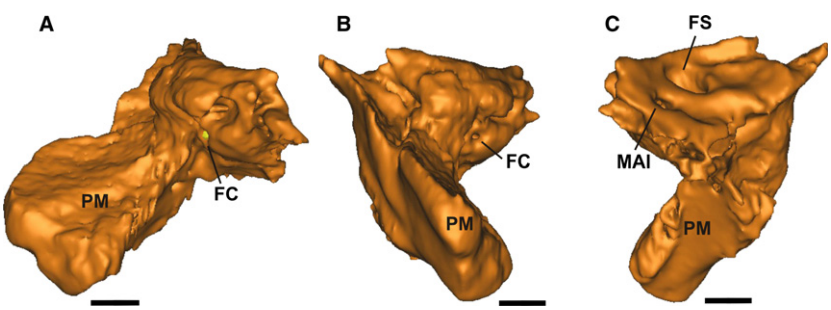

Fig. 4 Three-dimensional reconstruction of the right pars petrosa of the os temporale of *A. tarijense* (MACN 971). (A) anterior; (B) lateral and (C) medial views. FC, fenestra cochleae; FS, fossa subarcuata; MAI, meatus acusticus internus; PM, processus mastoideus. Scale bar: 1 cm.

The bony recess of the sacculus and the utriculus (= vestibular part of the inner ear) were also reconstructed. However, it was impossible to observe a discernible separation between them (Fig. 5). The cochlea is placed anterior to the canalis semicircularis and presents approximately three and a half spiral turns (counted following West, 1985) (Fig. 5A,B).

In the coronal view, the meatus acusticus internus is observed (Fig. 4C,D), which runs laterally and opens into two canals: one dorsal (the canalis facialis) for the passage of the nervi facialis (VII cranial nerve), and the other ventral (the canalis vestibulocochlearis) for the passage of the nervi vestibulocochlearis (VIII cranial nerve) (Fig. 5D). Near to the recessus epitympanicus and fenestra cochleae, the canalis facialis opens into a small recess which connects with the cavum tympani, so the nervi facialis passes through the inner and middle ear (auris interna and auris media) before emerging from the foramen

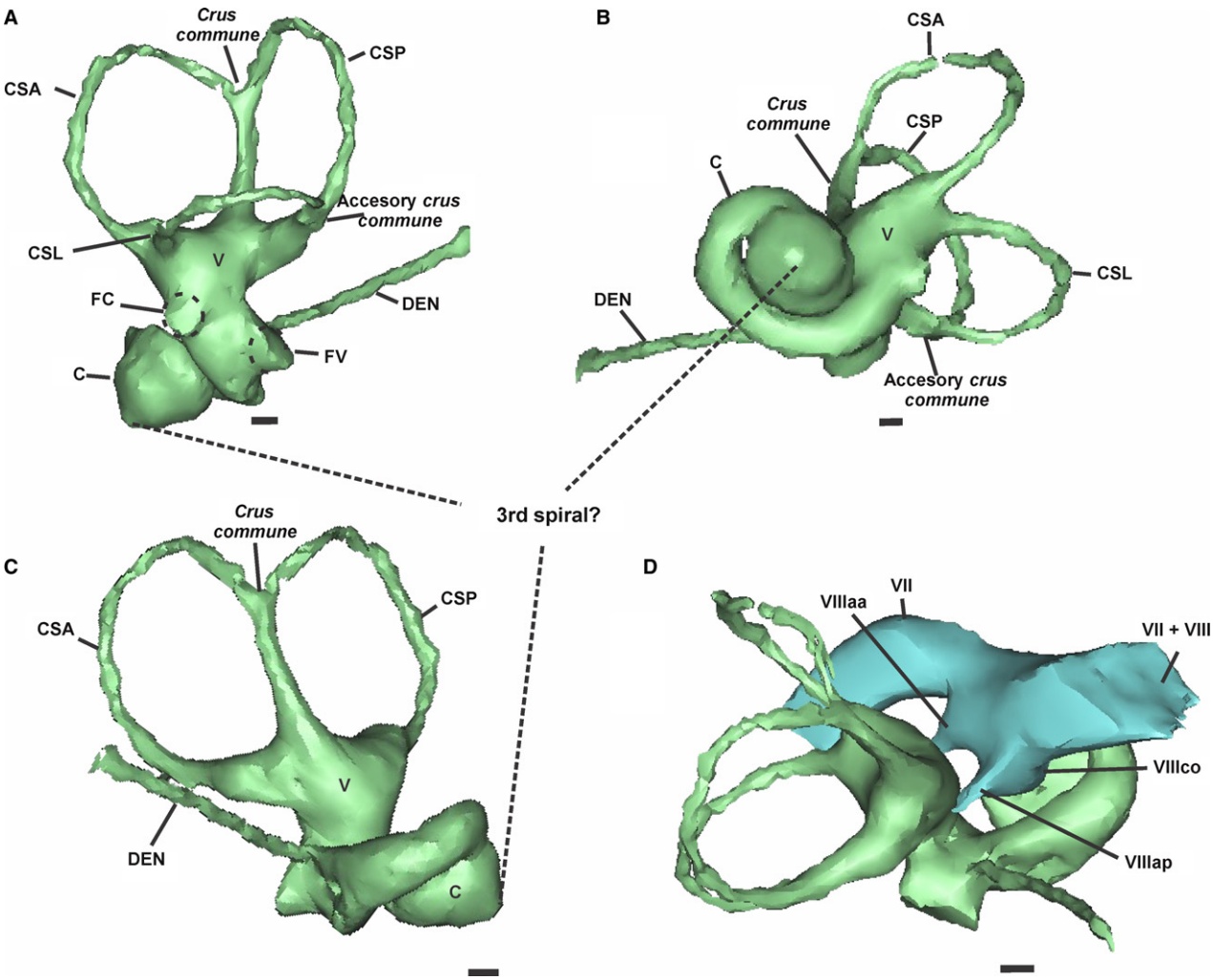

Fig. 5 Three-dimensional reconstruction of the left inner ear of *Arctotherium tarijense* (MACN 971). (A) Lateral; (B) anterior; (C) medial and (D) posteromedial views. C, cochlea; CSA, canalis semicircularis anterior; CSL, canalis semicircularis lateral; CSP, canalis semicircularis posterior; DEN, ductus endolymphaticus; FC, fenestra cochleae; FV, fenestra vestibuli; V, vestibule; VII, nervi facialis; VIII nervi vestibulocochlearis; VIIIaa, nervi ampularis anterior of the nervi vestibulocochlearis; VIIIap, nervi ampularis posterior of the nervi vestibulocochlearis; VIIIco, nervi cochlearis of the nervi vestibulocochlearis. Scale bar: 1 mm.

stylomastoideum (De Iuliis & Pulerà, 2007). In *A. tarijense*, the canalis vestibulocochlearis is divided in three branches, one thick and anterior, which opens into the cochlea for the passage of the nervi cochlearis, and other two posterior and smaller, which run dorsolaterally and enter into the base of the ampullae anteriorly (nervi ampullaris anterior) and posteriorly (nervi ampullaris posterior) (Meng & Fox, 1995; Macrini et al. 2010; Fig. 5D). The fenestra cochleae (fenestra rotunda) is an elliptical opening placed anterior and dorsal to the much larger fenestra vestibuli, as in most mammals (except in some notoungulates and some stem primates; Wible et al. 2007; Macrini et al. 2010) (Fig. 3C,D). This opening faces laterally and is covered by a secondary tympanic membrane in life. The fenestra vestibuli (fenestra ovalis) is an oval opening located ventral and medial to the accessory crus commune, in the posterior view, and is oriented obliquely (dorsoposterolateral to ventroanteromedial) relative to the horizontal plane of the skull. This opening faces ventrolaterally and holds the footplate of the stapes in mammals. The stapes is not preserved in this specimen, but the stapedial ratio was estimated (length/width of the fenestra vestibuli) as approximately 1.53.

Lateral to the fenestra vestibuli is the aqueductus vestibuli, which forms the canal for the passage of ductus endolymphaticus in life. It runs from the cochlea to the cavum cranii through the pars petrosa of the os temporale and opens into the medial surface of this bone (Fig. 5). As in *A. angustidens,* it is oriented anterolaterally to posteromedially. Unlike other mammals, such as marsupials (Schmelzle et al. 2007) or notoungulates (Macrini et al. 2010), in *A. tarijense* the diameters of the

aqueductus vestibuli and the canalis semicircularis are equal.

In *A. tarijense* the primary lamina of the cochlea is preserved (Fig. 3B,C). This bony structure serves as the conduit for the axons of hair cells and the spiral ganglion, and physically supports the medial margin of the basilar membrane. Thus, the primary lamina is the most reliable osteological correlate to infer the presence of modern therian-like cochlear innervations, and the extent of such innervations along the length of the cochlear canal (Luo et al. 2012). The bony primary spiral lamina curves along the modiolus (central bony pillar around which the cochlea coils) on the axial wall of the cochlea. The secondary lamina is also preserved in the opposing wall (radial) of the cochlea (Ekdale, 2009).

The anterior part of the pars petrosa of the os temporale is against but not fused to the tentorium cerebelli osseum (Fig. 6A). The pars petrosa contacts the exoccipital posteromedially and forms the processus mastoideus laterally. This process contacts the processus postglenoideus and the processus paraoccipitalis (Figs 1A,D,G and 6B). In the anteroventral part of the medial surface of the pars petrosa, the meatus acusticus internus and the fossa subarcuata open (Loza et al. 2015). This fossa housed the paraflocculus of the cerebellum (Wible et al. 1995), which is responsible for the control of the amplitude and timing of compensatory eye movements and the vestibulocular reflex (De Zeeuw et al. 2004). The fossa subarcuata passes through the arch delimited by the CSA and in *A. tarijense* occupies almost all the space between the three canalis semicircularis (Fig. 6C,D).

At the ventral surface of the pars petrosa of the os temporale of *A. tarijense* there are two depressions for muscular attachment (Torres, 1987): the fossa musculus tensor tympani (anterior) and the fossa musculus stapedialis (posterior). The fossa musculus tensor tympani is longer and deeper than the fossa musculus stapedialis, which is located posteroventral to the canalis facialis.

Following the orientation of the CSL, the orientation of the skull of *A. tarijense* in life shows an approximated inclination of 40° with respect to the horizontal plane (see Material and methods section).

Predicting head movements and locomotion

For *A. tarijense,* a body mass of 231 kg was estimated and the agility scores range from 2.72 to 2.88 (Table 1). The range of body masses estimated for this species were 250.9 kg (CR4), 218.6 kg (CR5) and 223.6 kg (CR6). *Arctotherium tarijense* and *T. ornatus* have the lowest values of orthogonality deviation (4. 90 and 4.71°, respectively).

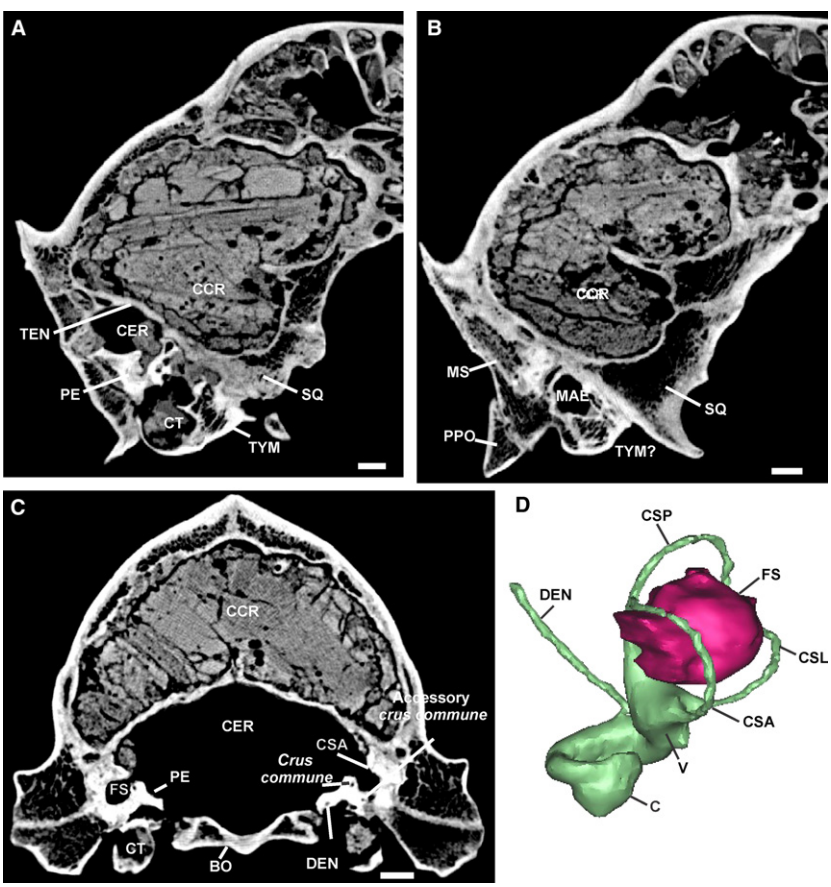

Fig. 6 *Arctotherium tarijense* (MACN 971). (A,B) CT sagittal images of the skull. (C) CT coronal image of the skull. (D) Three-dimensional reconstruction of the left inner ear. BO, pars basilaris os occipitale; C, cochlea; CER, cavum of the cerebellum; CCR, cavum cranii; CSA, canalis semicircularis anterior; CSL, canalis semicircularis lateral; CSP, canalis semicircularis posterior; CT, cavum tympani; DEN, ductus endolymphaticus; FS, fossa subarcuata; MAE, meatus acusticus externus; MS, mastoideus; PE, pars petrosa os temporale; PPO, processus paraoccipitalis; SQ, pars squamosa os temporale; TEN, tentorium cerebelli osseum; TYM, bulla tympanica; V, vestibule. Scale bar: 1 cm.

Discussion

Comparative anatomy

The external auditory region of *A. tarijense* differs from that in other tremarctines in its general shape and relative size. In this species, the bulla tympanica is slightly flat on the anterior margin, becoming globular posteriorly (Fig. 1A,D,G), producing a mostly globular appearance. It is much more globular than in any other Ursidae species (except for *A. wingei*). The cavum tympani in *A. tarijense* is also higher than in other tremartines. Comparing *A. tarijense* (a medium-sized species; skull volume of MACN 971 = 1465263.27 mm^3) with the larger *A. angustidens* (skull volume of MLP 82-X-22-1 = 3235289.37 mm^3), it is observed that the relationship of the cavum tympanii volume/skull volume $\times 100$ is approximately twice as large in *A. tarijense* (0.8%) as in *A. angustidens* (0.4%) (Fig. 2).

The basis cranii externa of *A. tarijense* is more similar to that in Ursinae (e.g. *U. arctos, U. maritimus, U. americanus, U. thibetanus)* than other tremarctines such as *A. angustidens*. Unlike *A. angustidens* (Arnaudo et al. 2014), in Ursinae the bulla tympanica contacts widely with the processus paraoccipitalis via a conspicuous ridge that separates the foramen stylomastoideum from the foramen jugulare. In other tremarctines, this ridge is less developed and therefore the foramen stylomastoideum lies in a common fossa with the foramen jugulare. This condition was described by Hough (1948) who generalized this for all tremarctines, but our results show that in *A. tarijense* this feature is different. Also, unlike *A. bonariense*, *A. pristinus, T. floridanus, T. ornatus,* and some specimens of *A. angustidens*, in *A. tarijense* the foramen postglenoideum is visible in lateral and ventral views. Other morphological differences in the basicranium of *A. tarijense* with other tremarctines are the presence of a small foramen at the ventral surface of the processus paraoccipitalis (Fig. 1) and the posteroventral orientation of the processus paraoccipitalis (this last condition is shared with *A. bonariense*).

In Ursidae the anterior region of the cavum tympani is partially divided into two (dorsal and ventral) recesses (Fig. 2) by an incomplete horizontal septum, which is the only septum present in bears at the middle ear (Arnaudo et al. 2014; see Flower, 1869 and Ivanoff, 2000 for a detailed description of the vertical and the transverse septum present in other Carnivora). The relative size of both recesses varies among bears: in *A. bonariense* they are similar in size, in *T. ornatus* and most Ursinae the dorsal is larger than the ventral (see Materials used for comparison), in *A. angustidens* the ventral is larger than the dorsal, and in *A. tarijense* the dorsal is extremely reduced (Fig. 2). In *A. tarijense* the recessus epitympanicus is small and practically undistinguished from the roof of the meatus acusticus externus, contrasting with the larger recessus epitympanicus observed in other Tremarctinae such as *A. angustidens*, *A. bonariense*, *T. floridanus* and *T. ornatus* (Figs 2 and 3B).

As stated above, the stapes is not preserved in the studied specimen. However, the estimated stapedial ratio of 1.53 for *A. tarijense* is lower than ratios reported for other placental mammals, which are typically greater than 1.8 (Segall, 1970). Segall (1970) pointed out that the round shape of the plate and fenestra ovalis (lower values of stapedial ratio) is a 'primitive' mammalian character and the elliptical shape (highest ratios), a 'specialized' (derived) one. As in *A. tarijense*, the stapedial ratio is low in some eutherians, such as some notoungulates (Macrini et al. 2010) and in most marsupials (Segall, 1970; Rougier et al. 1998; Horovitz et al. 2008).

The inner ear of *A. tarijense* also shows some differences with respect to other tremarctines. In relation to the spiral turns of the cochlea, the 3D model obtained from the CT scan of MACN 971 shows approximately two and half spiral turns (probably three?; Fig. 5A–C). Given the low resolution of the CT scans (see Material and methods), in *A. angustidens* it was possible to identify only two turns of the spiral cochlea (Arnaudo et al. 2014). The canalis semircularis of *A. tarijense* shows the structure typical of mammals, and they do not show marked differences within the other members of the family. The CSP and the CSA have the same height, a pattern typical for quadrupedal vertebrates (Spoor & Zonneveld, 1998; Witmer et al. 2003; Schmelzle et al. 2007; Fig. 5). The semicircular canal complex allows one to orientate the skull in life. Improving the head inclination could have helped to maintain a better visual field in tremarctines in relation to open areas (see Blanks et al. 1972; Spoor & Zonneveld, 1998; Witmer et al. 2003). Based on the relative position of the CSL, the skull (head) posture was more oblique in *Arctotherium. tarijense* (40°), *A. pristinus* (48°) and *T. floridanus* (38°) than in *A. angustidens* (32°), *A. bonariense* (24°) and *T. ornatus* (29°) (see above). The extant *T. ornatus* (which presents one of the lowest values of inclination of the head) lives in densely vegetated areas and, according to this, a high degree of inclination of the head, present in *A. tarijense* and *A. pristinus*, could have being related to a more accurate mode for long-distance vision.

Finally, here we report the presence of a secondary crus commune in the inner ear of *A. tarijense* and other ursids (i.e. *A. angustidens*, *A. bonariense*, *T. ornatus*, *U. spelaeus*, *U. americanus*, *U. maritimus* and *U. arctos;* see also Arnaudo et al. 2014), also reported for other mammals (Hyrtl, 1845; Meng & Fox, 1995; Sánchez-Villagra & Schmelzle, 2007; Macrini et al. 2010; Ruf et al. 2013). There is no hypothesis regarding the significance of the presence of this structure.

Head movements and locomotion

Although the postcranial skeleton of *A. tarijense* is unknown, here we propose some approaches to its

locomotor behavior based on the information obtained from its inner ear anatomy. In mammals it has been demonstrated that species with the greatest deviations from canal orthogonality tend to experience slower head rotations during locomotion and to have less sensitive semicircular canals (Malinzak et al. 2012; Berlin et al. 2013). As stated above, *A. tarijense* and *T. ornatus* have the lowest values of orthogonality deviation (4. 90 and 4.71°, respectively) and also show the highest scores of locomotor agility. In the same way *A. angustidens*, which is the largest tremarctine, has the highest orthogonality deviation and the lowest score of agility (Tables 1 and 2). Considering that the extant *T. ornatus* is a good climber and a relatively agile mammal, highest agility values might be expected for this species. *Tremarctos ornatus* inhabits different types of forest and high-elevation grasslands, being a species well adapted to closed-in habitats and an excellent climber. Although it appears that in bears the inferences based on agility scores should be viewed with much caution, the relatively high agility score of *A. tarijense* (higher than that of *U. arctos* and *U. maritimus*) could be related to a better ability to explore different kind of habitats.

Conclusions

Within Tremarctinae, *Arctotherium tarijense* shows major morphological differences in relation to the external and the internal morphology of the auditory bulla. Externally, we observed the following:

- *tarijense* shows the most globular tympanic bone, but it should be compared with *A. wingei* to obtain more accurate conclusions;
- the processus paraoccipitalis has a foramen which is absent in other tremarctines;
- there is a conspicuous bridge in the contact between the tympanic and the paraoccipital process, a feature shared with ursines.

At the middle ear, we observed the following:

- the cavum tympani of *A. tarijense* presents the highest relative volume compared with all bears in the sample, being twice the size of *A. angustidens* (in relation to the volume of the skull);
- in the anterior region of the cavum tympani there is only one (ventral) recess and the recessus epitympanicus is the smallest for all the ursids here studied.

Finally, in the inner ear, the cochlea seems to have more turns than in *A. angustidens*. However, the systematic value of these features should be tested in a phylogenetic analysis.

Although the radius of curvature of each semicircular canal (here expressed as locomotor agility) is important in estimating vestibular sensitivity in mammals, the orientations of all six canals also help to determine the relative sensitivity of the vestibular system to angular accelerations in three dimensions (Malinzak et al. 2012; Berlin et al. 2013). Based on the results here obtained, it is possible to make a preliminary proposal that *Arctotherium tarijense* had a relative high vestibular sensibility and therefore a better ability to explore different kind of habitats. However, this hypothesis should be contrasted among bears taking into account the orientation of each semicircular canal in a phylogenetic framework.

Acknowledgements

We thank Juan Pablo Merino from CIMED for his help with the CT scans. We thank Sharlene Wilds from Franklin Woods Community Hospital and other hospital staff for their assistance in the scanning process. We thank Thomas Macrini, Anthony Graham (Editor of *Journal of Anatomy*) and anonymous reviewer for valuable suggestions on early versions of this manuscript. We also thank the following persons and institutions for allowing the examination of their material: Marcelo Reguero, Museo de La Plata; Alejandro Kramarz, Museo Argentino de Ciencias Naturales 'Bernardino Rivadavia and Laura Gelari, Museo Histórico de Junín, República Argentina'. ANPCyT PICT 0804 BID and CONICET PIP 0496 are acknowledged for financial support. We acknowledge the Digital Morphology library (DIGIMORPH) at the University of Texas at Austin for access to CT scans housed at their library.

References

Ameghino F (1902) Notas sobre algunos mamíferos fósiles nuevos o poco conocidos del valle de Tarija. *An Mus Nac B Aires* **3**, 225–261.

Arnaudo ME, Soibelzon L, Bona P, et al. (2014) First Description of the auditory region of a Tremarctinae (Ursidae, Mammalia) Bear: The Case of *Arctotherium angustidens*. *J Mamm Evol* **21**, 321–330.

de Beaumont G (1968) Note sur la region auditive de quelques Carnivores. *Arch des Sci Genève* **21**, 211–224.

Berlin JC, Kirk EC, Rowe TB (2013) Functional implications of ubiquitous semicircular canal non-orthogonality in mammals. *PLoS One* **8**, e79585.

Billet G, Germain D, Ruf I, et al. (2013) The inner ear of *Megatherium* and the evolution of the vestibular system in sloths. *J Anat* **223**, 557–567.

Blanks RHI, Curthoys IS, Markham CH (1972) Planar relationships of semicircular canals in the cat. *Am J Physiol* **223**, 55–62.

Cox CB (1962) A natural cast of the inner ear of a dicynodont. *Am Mus Novit* **2116**, 1–6.

Davis DD (1964) The giant panda. A morphological study of evolutionary mechanism. *Fieldiana Zool Mem* **3**, 1–399.

De Iuliis G, Pulerà D (2007) *The Dissection of Vertebrates: A Laboratory Manual*, 1st edn. Oxford: Elsevier.

De Zeeuw C, Koekkoek SK, Van Alphen AM, et al. (2004) Gain and phase control of compensatory eye movements by the flocculus of the vestibulo-cerebellum. In: *Handbook of Auditory Research* (eds Highstein SM, Fay RR, Popper AN), pp. 375–422. New York: Springer.

Eisenberg JF (1989) An introduction to the Carnivora. In: *Carnivore Behavior, Ecology, and Evolution* (ed. Gittleman JL), pp. 1–9. Ithaca, NY: Cornell University Press.

Ekdale EG (2009) Variation within the bony labyrinth of mammals. PhD Dissertation. University of Texas, Austin.

Ekdale EG (2013) Comparative anatomy of the bony labyrinth (inner ear) of placental mammals. *PLoS One* **8**, e66624.

Ekdale EG (2016) Form and function of the mammalian inner ear. *J Anat* **228**, 324–337.

Ekdale EG, Rowe T (2011) Morphology and variation within the bony labyrinth of zhelestids (Mammalia, Eutheria) and other therian mammals. *J Vertebr Paleontol* **3**, 658–675.

Flower WH (1869) On the value of the characters of the base of the skull in the classification of the Order Carnivora, and on the systematic position of Bassaris and other disputed forms. *Proc Zool Soc Lond* **37**, 4–37.

Ginsburg L (1966) Les amphicyons des Phosphorites du Quercy. *Ann Paléontol* **52**, 23–64.

Horovitz I, Ladevèze S, Argot C, et al. (2008) The anatomy of *Herpetotherium fugax* Cope 1873, a metatherian from the Oligocene of North America. *Palaeontographica Abt A* **284**, 109–141.

Hough JR (1948) The auditory region in some members of the Procyonidae, Canidae, and Ursidae. Its significance in the phylogeny of the Carnivora. *Bull Am Mus Nat Hist* **92**, 67–118.

Hough JR (1952) Auditory region in North American Felidae: significance in phylogeny. *Geol Surv Prof Pap* **243**, 95–115.

Hunt RM Jr (1974) The auditory bulla in Carnivora: an anatomical basis for reappraisal of carnivore evolution. *J Morphol* **143**, 21–76.

Hyrtl J (1845) *Vergleichend-Anatomische Untersuchungen über das innere Gehörorgan des Menschen und der Säugethiere*. Prague: Friedrich Ehrlich.

Ivanoff DV (2000) Origin of the septum in the canid auditory bulla: evidence from morphogenesis. *Acta Theriol* **45**, 253–270.

Kurtén B (1966) Pleistocene bears of North America: 1. Genus *Tremarctos*, spectacled bears. *Acta Zool Fenn* **115**, 1–120.

Kurtén B (1967) Pleistocene bears of North America: 2. Genus *Arctodus*, short faced bears. *Acta Zool Fenn* **117**, 1–60.

Ladevèze S, Asher RJ, Sánchez-Villagra MR (2008) Petrosal anatomy in the fossil mammal *Necrolestes*: evidence for metatherian affinities and comparisons with the extant marsupial mole. *J Anat* **213**, 686–697.

Ladevèze S, De Muizon C, Colbert M, et al. (2010) 3D computational imaging of the petrosal of a new multituberculate mammal from the Late Cretaceous of China and its paleobiologic inferences. *CR Palevol* **9**, 319–330.

Loza CM, Scarano AC, Soibelzon LH, et al. (2015) Morphology of the tympanic-basicranial region in *Mirounga leonina* (Phocidae, Carnivora), postnatal ontogeny and sexual dimorphism. *J Anat* **226**, 354–372.

Luo ZX, Ruf I, Schultz JA, et al. (2011) Fossil evidence on evolution of inner ear cochlea in Jurassic mammals. *Proc R Soc B* **278**, 28–34.

Luo ZX, Ruf I, Martin T (2012) The petrosal and inner ear of the Late Jurassic cladotherian mammal *Dryolestes leiriensis* and implications for ear evolution in therian mammals. *Zool J Linn Soc* **166**, 433–463.

Macrini TE, Flynn JJ, Croft DA, et al. (2010) Inner ear of a notoungulate placental mammal: anatomical description and examination of potentially phylogenetically informative characters. *J Anat* **216**, 600–610.

Malinzak MD, Kay RF, Hullar TE (2012) Locomotor head movements and semicircular canal morphology in primates. *Proc Natl Acad Sci U S A* **109**, 17914–17919.

Meng J, Fox RC (1995) Osseous inner ear structures and hearing in early marsupials and placentals. *Zool J Linn Soc* **115**, 47–71.

Nomina Anatomica Veterinaria (2012) *International Committee on Veterinary Gross Anatomical Nomenclature*. 5th edn. Ithaca, NY: Department of Veterinary Anatomy, Cornell University.

Orliac MJ, Benoit J, O'Leary MA (2012) The inner ear of *Diacodexis*, the oldest artiodactyl mammal. *J Anat* **221**, 417–426.

Pocock RI (1921) The external characters and classification of the Procyonidae. *Proc Zool Soc Lond* **91**, 389–422.

Pocock RI (1922) The external characters and classification of the Mustelidae. *Proc Zool Soc Lond* **91**, 803–837.

Pocock RI (1929) The structure of the auditory bulla in the Procyonidae and the Ursidae, with a note on the bulla of Hyaena. *Proc Zool Soc Lond* **98**, 963–974.

Rodrigues PG, Ruf I, Schultz CL (2013) Digital reconstruction of the otic region and inner ear of the non-nammalian cynodont *Brasilitherium riograndensis* (late triassic, Brazil) and its relevance to the evolution of the mammalian ear. *J Mamm Evol* **20**, 291–307.

Rougier GW, Wible JR, Novacek MJ (1998) Implications of *Deltatheridium* specimens for early marsupial history. *Nature* **396**, 459–463.

Ruf I, Luo ZX, Martin T (2013) Reinvestigation of the basiskull of *Haldanodon exspectatus* (Mammaliaformes, Docodonta). *J Vertebr Paleontol* **33**, 382–400.

Ryan TM, Silcox MT, Walker A, et al. (2012) Evolution of locomotion in Anthropoidea: the semicircular canal evidence. *Proc R Soc Lond B Biol Sci* **279**, 3467–3475.

Sánchez-Villagra MR, Schmelzle T (2007) Anatomy and development of the bony inner ear in the woolly opossum, *Caluromys philander* (Didelphimorphia, Marsupialia). *Mastozool Neotrop* **14**, 53–60.

Schmelzle T, Sánchez-Villagra MR, Maier W (2007) Vestibular labyrinth evolution in diprotodontian marsupial mammals. *Mamm Stud* **32**, 83–97.

Schubert B (2010) Late Quaternary chronology and extinction of North American short-faced bears (*Arctodus simus*). *Quat Int* **217**, 188–194.

Segall W (1943) The auditory region of the arctoid carnivores. *Zool Ser Field Mus Nat Hist* **29**, 33–59.

Segall W (1970) Morphological parallelisms of the bulla and auditory ossicles in some insectivores and marsupials. *Fieldiana Zool* **51**, 169–205.

Silcox MT, Bloch JI, Boyer DM, et al. (2009) Semicircular canal system in early primates. *J Hum Evol* **56**, 315–327.

Smith RJ (1993) Bias in equations used to estimate fossil primate body mass. *J Hum Evol* **43**, 271–287.

Soibelzon LH (2004) Revisión sistemática de los Tremarctinae (Carnivora, Ursidae) fósiles de América del Sur. *Rev Mus Argent Cienc Nat* **6**, 107–133.

Soibelzon LH, Schubert BW (2011) The largest known bear, *Arctotherium angustidens*, from the early Pleistocene Pampean Region of Argentina: with a discussion of size and diet trends in bears. *J Paleontol* **85**, 69–75.

Soibelzon LH, Tartarini VB (2009) Estimación de la masa corporal de las especies de osos fósiles y actuales (Ursidae, Tremarctinae) de América del Sur. *Rev Mus Argent Cienc Nat* **11**, 243–254.

Soibelzon LH, Tonni EP, Bond M (2005) The fossil record of South American short-faced bears (Ursidae, Tremarctinae). *J South Am Earth Sci* **20**, 105–113.

Spoor F (2003) The semicircular canal system and locomotor behaviour, with special reference to hominin evolution. *Courier Forschungsinstitut Senckenberg* **243**, 93–104.

Spoor F, Zonneveld F (1998) Comparative review of the human bony labyrinth. *Yearb Phys Anthr* **41**, 211–251.

Spoor F, Garland T, Krovitz G, et al. (2007) The primate semicircular canal system and locomotion. *Proc Natl Acad Sci USA* **104**, 10808–10812.

Tedford RH, Martin J (2001) *Plionarctos*, a tremarctinae bear (Ursidae: Carnivora) from western North America. *J Vertebr Paleontol* **21**, 311–321.

Thenius E (1949) Zur Revision der Insektivoren des steirischen Tertiars II. *Sitzungsberichte der Österrischen Akad, Wissensch mathnaturwissensch Klasse, Abt I* **159**, 671–693.

Torres T (1984) Los Úrsidos del Pleistoceno- Holoceno de la Península Ibérica. Madrid: Tesis Doctoral Escuela Técnica Superior de Ingenieros de Minas de Madrid.

Torres T (1987) La región auditiva en los Osos del Pleistoceno europeo. *Rev Esp Paleontol* **2**, 41–47.

Torres T (1988) Osos (Mammalia, Carnivora, Ursidae) del Pleistoceno de la Península Ibérica. *Publicación especial del Boletín Geológico y Minero, Instituto Geológico y Minero de España* **94**, 1–316.

Turner HN (1848) Observations relating to some of the foramina at the base of the skull in Mammalia; and on the classification of the Order Carnivora. *Proc Zool Soc Lond* **16**, 63–88.

Van Der Klaauw CJ (1931) The auditory region of some fossil mammals with a general introduction to this region of the skull. *Bull Am Mus Nat Hist* **62**, 1–352.

Van Kampen PN (1905) Die Tympanalgegend des Säugetierschädels. *Morphol Jahrb* **34**, 321–722.

Van Valkenburgh B (1990) Skeletal and dental predictors of body mass in carnivores. In: *Body Size in Mammalian Paleobiology: Estimation and Biological Implications* (eds Damuth J, MacFadden BJ), pp. 181–206. New York: Cambridge University Press.

Walker A, Ryan TM, Silcox MT, et al. (2008) The semicircular canal system and locomotion: the case of extinct lemuroids and lorisoids. *Evol Anthrop* **17**, 135–145.

West CD (1985) The relationship of the spiral turns of the cochlea and the length of the basilar membrane to the range of audible frequencies in ground dwelling mammals. *J Acoust Soc Am* **77**, 1091–1101.

Wible JR, Rougier RW, Novacek MJ, et al. (1995) A mammalian petrosal from the Early Cretaceous of Mongolia: Implications for the evolution of the ear region and mammaliamorph interrelationships. *Am Mus Novit* **3149**, 19.

Wible JR, Rougier GW, Novacek MJ, et al. (2007) Cretaceous eutherians and Laurasian origin for placental mammals near the K/T boundary. *Nature* **447**, 1003–1006.

Witmer LM, Chatterjee S, Franzosa J, et al. (2003) Neuroanatomy of flying reptiles and implications for flight, posture and behavior. *Nature* **425**, 950–953.

Wozencraft WC (1989) The phylogeny of the recent Carnivora. In: *Carnivore Behavior, Ecology, and Evolution* (ed. Gittleman JL), pp. 495–535. Ithaca, NY: Cornell University Press.

Wozencraft WC (2005) Order Carnivora. In: *Mammal Species of the World*, 3rd edn (eds Wilson DE, Reeder DM), pp. 532–628. Baltimore: The Johns Hopkins University Press.

Wyss AR, Flynn JJ (1993) A phylogenetic analysis and definition of the Carnivora. In: *Mammal Phylogeny: Placentals* (eds. Szalay FS, Novacek MJ, McKenna MC), pp. 32–52. New York: Springer-Verlag.